



# Synthesis, thermal and photophysical studies of $\pi$ -extended dibenzophenazine based discotic liquid crystals

Litwin Jacob<sup>a,1</sup>, Ashwathanarayana Gowda<sup>a,1</sup>, Sandeep Kumar<sup>a,b,\*</sup>, Victor Belyaev<sup>c,d</sup>

<sup>a</sup> Raman Research Institute, C.V. Raman Avenue, Sadashivanagar, Bangalore 560 080, India

<sup>b</sup> Department of Chemistry, Nitte Meenakshi Institute of Technology (NMIT), Yelahanka, Bangalore 560 064, India

<sup>c</sup> Moscow Region State University, Moscow, Russia

<sup>d</sup> RUDN University (People's Friendship University of Russia), Moscow, Russia

## ARTICLE INFO

### Article history:

Received 3 July 2020

Received in revised form 19 September 2020

Accepted 22 September 2020

Available online 28 September 2020

### Keywords:

Dibenzophenazine

Discotic liquid crystals

Columnar phase

Sonogashira coupling

## ABSTRACT

Novel  $\pi$ -extended dibenzophenazine based discotic mesogens tethered with alkane thiols and alkoxy phenylacetylene along with alkoxy chains have been designed and synthesised. Molecular structures of all compounds were investigated using spectral and elemental analysis. The liquid crystalline properties of all the novel compounds were characterized using polarised optical microscopy (POM) and differential scanning calorimetry (DSC). The self-assembly of mesophase structure of discotic mesogens were examined with the help of X-ray diffraction studies. All compounds exhibit stable hexagonal columnar mesophase over broad temperature range. The photophysical properties of these compounds were studied in anhydrous chloroform solvent at room temperature which exhibit absorption at 446–463 nm and corresponding emission at 578–600 nm. The high delocalization of  $\pi$ -electrons in extended dibenzophenazine discotic mesogens may find potential applications in devices like, solar cells, sensors, organic light emitting diodes, thin film transistors, etc.

© 2020 Elsevier B.V. All rights reserved.

## 1. Introduction

Molecular shape anisotropy is among the important key factors which determine the self-organization of molecules into liquid crystalline phases [1,2]. The generation of self-healing and self-aligning ability of liquid crystals can be easily architecture through nano-segregation of incompatible molecular subunits driven by the non-covalent weak interactions such as hydrogen bonding, van der Waals forces,  $\pi$ - $\pi$  interactions, dipole-dipole interaction and charge transfer interactions etc. [3–7]. They have application potential as novel anisotropic advanced functional materials for technological devices [8–13]. In this regard, discotic liquid crystals (DLCs) have been attracted considerable attention due to the formation of self-assembled ordered columnar structures [9–16]. The self-assembly of columnar structures is mainly controlled by the stacking arrangement of disc shape molecules. The molecular designing of discotic liquid crystals consisting of a flat, rigid aromatic disc-like  $\pi$ -conjugated structure surrounded by insulating mantle of flexible aliphatic chains. The formation of columnar structure is depends on supramolecular interactions of discotic mesogens [17–20]. They commonly exhibit two general classes of mesophase

structures. The self-assembly of discotic mesogens with only orientational order exhibits discotic nematic ( $N_D$ ) phase. The  $N_D$  phase is less commonly observed mesophase structure but it finds immense application as an optical compensating film to enlarge wide-viewing angle in the display devices [21–25]. The self-organized columnar mesophases are formed when individual anisotropic discotic mesogens stack one on top of the other to form one-dimensional columnar arrangement and lattice arrangement of columns defines the subclass of mesophase structure [26]. The large  $\pi$ - $\pi$  overlap between adjacent aromatic cores paves the road map for migration of charges along the columnar axis [2]. Due to this peculiar behaviour, DLCs have found applications in optoelectronic device applications such as organic light emitting diodes (OLEDs) [27–29], organic field effect transistors (OEFT) [30–33], photovoltaic solar cells [34,35] and sensors [36,37].

The presence of heterocyclic core unit in the discotic liquid crystals is associated with their strong dipole moment, electron deficiency, etc., which enhance the electron transport properties for advanced materials in semiconducting devices. Phenazine based heterocyclic compounds have found applications in photophysical and biological sciences [38–40]. The phenazine fused phenanthrene core leads to the construction of dibenzo[a,c]phenazine heteroaromatic polycyclic compounds. William et al. reported the tetraalkoxy dibenzophenazine based discotic liquid crystals containing monomeric acid and ester derivatives. The monomeric acid derivatives form H-bonded dimers which lead to elliptical shape structure and exhibit hexagonal columnar, rectangular and

\* Corresponding author at: Raman Research Institute, C.V. Raman Avenue, Sadashivanagar, Bangalore 560 080, India.

E-mail address: [skumar@rri.res.in](mailto:skumar@rri.res.in) (S. Kumar).

<sup>1</sup> Contributed equally to this work.

nematic phases over broad temperature [41]. Subsequently, they also prepared several tetraalkoxydibenzo[*a,c*]phenazines based DLC derivatives containing electron donating and electron withdrawing functional groups present at the phenazine ring. Phenazine mesogens with electron withdrawing functional groups exhibit stable Col<sub>h</sub> phase over broad temperature but phenazine ring containing electron donating groups does not show any liquid crystalline behaviour [42]. Detail investigations on the position of acid, ester and nitro functional groups on mesomorphic properties of tetraalkoxydibenzo[*a,c*]phenazines have been reported [43]. Further, the dimers of tetraalkoxydibenzo[*a,c*]phenazine linking through flexible alkyl chains which self-assemble one on top of other to form double-decker architecture and exhibit mesomorphic properties have been realized [44]. Recently, Ong and co-workers reported the synthesis and mesomorphic properties of hexaalkoxydibenzo[*a,c*]phenazines derivatives which exhibit Col<sub>h</sub> phase over broad temperature [45]. They also reported synthesis and thermal properties of non-mesomorphic tetraalkoxydibenzo[*a,c*]phenazines bearing lateral metal free crown ether. However, complexation of sodium metal crown ether containing tetraalkoxydibenzo[*a,c*]phenazines exhibit a rectangular columnar phase with *C2mm* symmetry [46]. Paulina and co-workers investigated the gelation and photophysical properties of monomeric acid and its corresponding monomeric ester derivatives of dibenzophenazine and diphenylquinoxaline based DLCs. The acid and ester derivatives of dibenzophenazine exhibit mesomorphic properties, however, the acid and ester derivatives of diphenylquinoxaline do not form LC phase because of aromatic rings are more flexible. The acid derivatives exhibit gelation properties in nonpolar solvents due to H-bonding [47].

In this article, we report the design and synthesis of some novel  $\pi$ -extended dibenzophenazine based heterocyclic discotic liquid crystals. Three series of extended tetraalkoxydibenzo[*a,c*]phenazines based DLCs containing a lateral substitution of alkanethiols, symmetrical and un-symmetrical substitution of 4-alkoxy phenylacetylene groups have been synthesised and investigated for their liquid crystalline properties. The intermediate and final compounds exhibit wide range of stable columnar mesophase. We discuss the synthesis, liquid crystalline characterisation and photophysical properties of extended heterocyclic DLCs. The molecular structures of intermediate and final compounds were characterized by spectral and elemental analysis. The mesomorphic properties were investigated using polarised optical microscopy (POM), differential scanning calorimetry (DSC). The self-assembly of mesophase structure was investigated with help of X-ray diffraction (XRD) studies. The photophysical properties were investigated using UV-Vis and emission spectroscopy.

## 2. Results and discussion

### 2.1. Synthesis and characterisation

The synthetic plan of novel dibenzophenazine based DLCs is shown in Scheme 1. The 1,2-bis(3,4-bis(dodecylperoxy)phenyl)ethane-1,2-dione intermediate **2** was synthesised following reported procedure [48] and it was condensed with 4,5-dibromobenzene-1,2-diamine **3** [49] in presence of glacial acetic acid under reflux condition affording tetraalkoxy substituted dibromoquinoxaline compound **4**. An intramolecular Scholl reaction was carried in presence of iron (III) chloride to furnish the tetraalkoxy substituted dibromo-dibenzophenazine key intermediate **5**. The reaction of alkanethiols with **5** in presence of cesium carbonate gives thiolated tetraalkoxydibenzo[*a,c*]phenazines (**6a–6c**) DLCs. Further, Sonagashira coupling reaction of intermediate **5** with 4-alkoxy phenylacetylene [50] in presence of bis (triphenylphosphine)palladium chloride (PdCl<sub>2</sub>(PPh<sub>3</sub>)<sub>2</sub>) and copper iodide (CuI) gives final  $\pi$ -extended dibenzophenazine based DLCs compounds (**7a–7d** and **8a–8c**). All intermediate and final compounds were purified by column chromatography and recrystallized from appropriated solvent to ensure maximum purity of the compounds. The

molecular structures of all compounds were characterized using IR, <sup>1</sup>H NMR, <sup>13</sup>C NMR and elemental analysis.

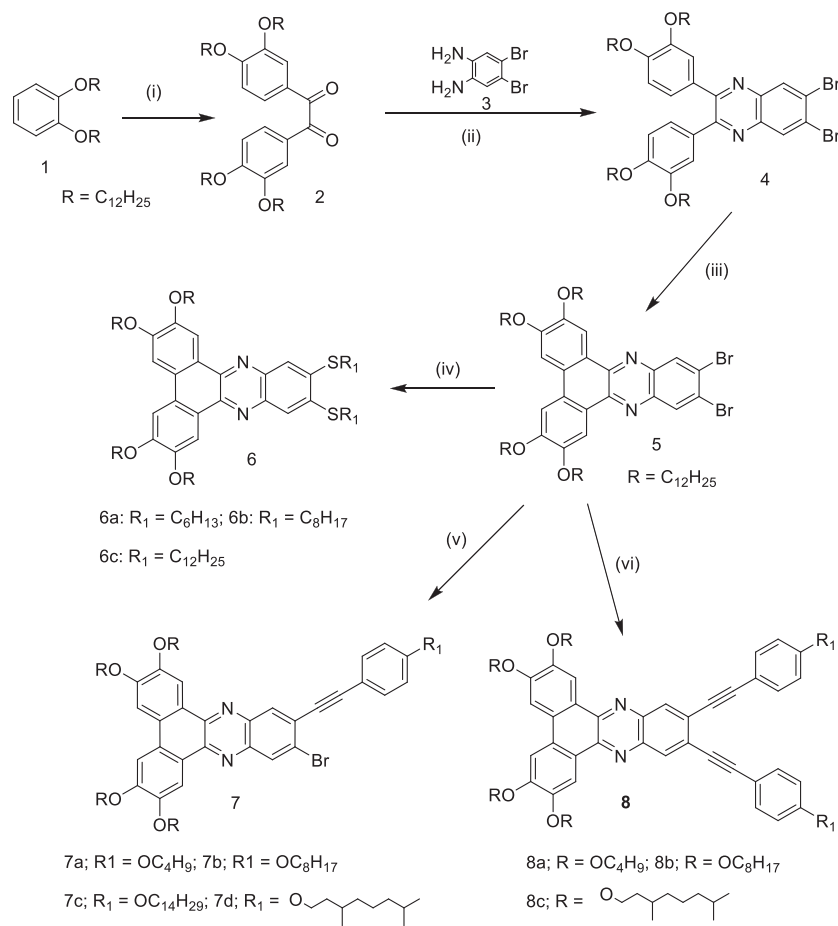
### 2.2. Thermal properties

Thermotropic liquid crystalline properties of all intermediate and final dibenzophenazine DLC derivatives are summarized in Table 1. The phase transition temperature (peak temperature in °C) and associated enthalpy ( $\Delta H$  in kJ mol<sup>-1</sup>) values obtained from the heating and subsequent cooling cycles of respective mesogens were determined by DSC. The columnar textures of mesogens observed using the POM as shown in Fig. 1.

The intermediate compound **5** was crystalline at room temperature and melts to mesophase at 103.1 °C along with enthalpy of phase transition ( $\Delta H$ ) of 45.01 kJ mol<sup>-1</sup>, which further transferred to isotropic liquid at 150.2 °C ( $\Delta H = 1.93$  kJ mol<sup>-1</sup>). Upon cooling, under POM, the appearance of mosaic textures revealed the formation of hexagonal columnar phase at 148.1 °C (ESI, Figs. S1a and S2). The thiol substituted final mesogenic compounds (**6a–6c**) exhibit enantiotropic hexagonal columnar mesophase over broad temperature. Compound **6a**, upon heating melts at 55.1 °C with phase transition enthalpy ( $\Delta H = 62.55$  kJ mol<sup>-1</sup>) to hexagonal columnar phase and become isotropic liquid at 121.1 °C ( $\Delta H = 5.01$  kJ mol<sup>-1</sup>) (ESI, Fig. S3). On cooling from the isotropic liquid, it exhibits typical textures of Col<sub>h</sub> phase at 118.4 °C under POM and become crystals at 24.3 °C ( $\Delta H = -63.26$  kJ mol<sup>-1</sup> in DSC). As a representative example of POM texture obtained for compounds, **6a** is shown in Fig. 1(a). Further, compounds **6b** and **6c** also exhibit similar trends of phase transitions from crystalline phase to Col<sub>h</sub> phase at 77.3 °C ( $\Delta H = 26.46$  kJ mol<sup>-1</sup>) and 100.2 °C ( $\Delta H = 29.25$  kJ mol<sup>-1</sup>) respectively and Col<sub>h</sub> to isotropic liquid at 135.5 °C ( $\Delta H = 3.42$  kJ mol<sup>-1</sup>) and 129.2 °C ( $\Delta H = 3.02$  kJ mol<sup>-1</sup>) respectively (ESI Fig. S4). On cooling from the isotropic liquid, the Col<sub>h</sub> phase occurred at 132.8 °C ( $\Delta H = -3.50$  kJ mol<sup>-1</sup>) and 126.9 °C ( $\Delta H = -2.89$  kJ mol<sup>-1</sup>) respectively. The DSC thermogram of representative compound **6c** is shown in Fig. 2a.

The unsymmetrically substituted  $\pi$ -extended dibenzophenazine based DLCs (**7a–7d**) exhibit similar trends of phase transition from crystalline phase to Col<sub>h</sub> at lower temperature and Col<sub>h</sub> phase to isotropic phase at higher temperature. Compound **7a** melts to Col<sub>h</sub> at 73.7 °C along phase transition enthalpy 32.88 kJ mol<sup>-1</sup> and become isotropic liquid at 174.7 °C ( $\Delta H = 2.0$  kJ mol<sup>-1</sup>) (ESI Fig. S5). The mesophase texture was observed upon slow cooling from isotropic liquid at 171.6 °C ( $\Delta H = -2.0$  kJ mol<sup>-1</sup>). As a representative example of POM texture obtained for compounds, **7a** is shown in Fig. 1(b). Compounds **7b** displayed similar phase transition from Cr to Col<sub>h</sub> at 71.9 °C ( $\Delta H = 25.63$  kJ mol<sup>-1</sup>) and Col<sub>h</sub> to isotropic phase at 152.4 °C ( $\Delta H = 0.92$  kJ mol<sup>-1</sup>) (ESI Fig. S6). The appearance of columnar texture was observed under POM at 148.9 °C ( $\Delta H = -0.96$  kJ mol<sup>-1</sup>) (on cooling) and become crystal phase at 14 °C (ESI Fig. S1b). The higher homologue, compound **7c**, having tetradecane alkyl chain shows monotropic phase transition. Upon heating, compound **7c** directly transferred into isotropic phase at 79.6 °C ( $\Delta H = 28.08$  kJ mol<sup>-1</sup>) (ESI Fig. S7), whereas upon cooling, dendritic textures were observed under POM at 62 °C as shown in ESI Fig. S1c. The phase transition from isotropic phase to Col<sub>h</sub> phase occurred at 79.5 °C ( $\Delta H = -0.35$  kJ mol<sup>-1</sup>). Compound **7d** with branched alkyl chains displayed Cr to Col<sub>h</sub> phase transition at 59.3 °C ( $\Delta H = 25.33$  kJ mol<sup>-1</sup>), which further become clear liquid at 146.3 °C ( $\Delta H = 1.18$  kJ mol<sup>-1</sup>) (ESI Fig. S8). On slow cooling from the isotropic liquid, under POM, show appearance of dendritic textures at 143.4 °C ( $\Delta H = -1.14$  kJ mol<sup>-1</sup>).

The symmetrically substituted  $\pi$ -extended dibenzophenazine based DLCs (**8a–8c**) also exhibit hexagonal columnar mesophase over broad temperature. Compounds **8a** and **8b** displayed Cr to Col<sub>h</sub> phase at 82.1 °C ( $\Delta H = 30.38$  kJ mol<sup>-1</sup>) and 77.2 °C ( $\Delta H = 29.37$  kJ mol<sup>-1</sup>) respectively, which further transferred to the isotropic liquid at 181.1 °C ( $\Delta H = 0.59$  kJ mol<sup>-1</sup>) and 164.9 °C ( $\Delta H = 0.94$  kJ mol<sup>-1</sup>) respectively



**Scheme 1.** (i) Oxalyl chloride, anhy.  $AlCl_3$ , DCM, r.t., 12 h; (ii) glacial acetic acid, reflux, 6 h; (iii)  $FeCl_3$ , r.t., 6 h; (iv) alkanethiol,  $CS_2CO_3$ , DMAC, reflux, 24 h; (v) & (vi) 1-ethynyl-4-alkoxybenzene,  $PdCl_2(PPh_3)_2$ , CuI, TEA, reflux, 24 h.

(ESI Fig. S9). On slow cooling, they displayed columnar texture under POM at 178.2 °C ( $\Delta H = -0.45 \text{ kJ mol}^{-1}$ ) and 161.5 °C ( $\Delta H = -0.89 \text{ kJ mol}^{-1}$ ), respectively. A representative DSC thermogram of compound **8b** is shown in Fig. 2(b). Similarly, compound **8c** undergoes Cr to  $Col_h$  phase at 60.1 °C ( $\Delta H = 22.52 \text{ kJ mol}^{-1}$ ) and become clear liquid at 158.9 °C ( $\Delta H = 0.59 \text{ kJ mol}^{-1}$ ) (ESI Fig. S10). On slow cooling under POM show the appearance of dendritic textures at 153.9 °C ( $\Delta H = -0.57 \text{ kJ mol}^{-1}$ ) and crystallize at around room temperature 30.5 °C ( $\Delta H = -21.72 \text{ kJ mol}^{-1}$ ) (ESI Fig. S1d). The thiolalkyl

**Table 1**

Phase transition temperature obtained from DSC (peak in DSC °C) and enthalpies ( $\text{kJ mol}^{-1}$ , in parentheses) of all the mesogens **5**, **6a–6c**, **7a–7d** and **8a–8c** (on heating and cooling cycle). Cr = crystalline phase;  $Col_h$  = hexagonal columnar phase; I = isotropic phase.

Compound	Phase transition peak temperature (°C); ( $\Delta H$ , [ $\text{kJ mol}^{-1}$ ])	
	Second heating scan	Second cooling scan
<b>5</b>	Cr 103.1 [45.01] $Col_h$ 150.2 [1.93] I	I 148.1 [−1.87] $Col_h$ 74.1 [−42.29] Cr
<b>6a</b>	Cr 55.1 [62.55] $Col_h$ 121.1 [5.01] I	I 118.4 [−4.85] $Col_h$ 24.3 [−63.26] Cr
<b>6b</b>	Cr 77.3 [26.46] $Col_h$ 135.5 [3.42] I	I 132.8 [−3.50] $Col_h$ 45.32 [−27.27] Cr
<b>6c</b>	Cr 100.2 [29.25] $Col_h$ 129.2 [3.02] I	I 126.9 [−2.89] $Col_h$ 67.6 [−32.91] Cr
<b>7a</b>	Cr 73.7 [32.88] $Col_h$ 174.7 [2.0] I	I 171.6 [−2.0] $Col_h$ 9.7 [−18.12] Cr
<b>7b</b>	Cr 71.9 [25.63] $Col_h$ 152.4 [0.92] I	I 148.9 [−0.96] $Col_h$ 14.4 [−20.28] Cr
<b>7c</b>	Cr 79.6 [28.08] I	I 79.5 [−0.35] $Col_h$ 39.6 [−29.38] Cr
<b>7d</b>	Cr 59.3 [25.33] $Col_h$ 146.3 [1.18] I	I 143.4 [−1.14] $Col_h$ 18.6 [−23.52] Cr
<b>8a</b>	Cr 82.1 [30.38] $Col_h$ 181.1 [0.59] I	I 178.2 [−0.45] $Col_h$ 55.4 [−32.38] Cr
<b>8b</b>	Cr 77.2 [29.37] $Col_h$ 164.9 [0.94] I	I 161.5 [−0.89] $Col_h$ 44.5 [−28.82] Cr
<b>8c</b>	Cr 60.1 [22.52] $Col_h$ 158.9 [0.59] I	I 153.9 [−0.57] $Col_h$ 30.5 [−21.72] Cr

substituted dibenzophenazine derivatives exhibit mesophase to isotropic phase transition at low temperature. However, symmetrical and unsymmetrical substituted  $\pi$ -extended dibenzophenazine having large core size exhibit mesophase to isotropic phase transition at high temperature. This implies that increasing core size leads to a greater propensity to form stable columnar mesophase, which is consistent with the literature report that larger discotic mesogens tend to form liquid crystal phases over broad temperature [51–54]. Williams et al. reported that the addition of electron-withdrawing groups should lead to an increase in the molecular dipole moment, which will favor the antiparallel orientation of adjacent molecules within the columns. In our case, the dibenzophenazine derivatives containing alkoxy chains and thioalkyl chains exhibit stable columnar phase where discotic cores are self-assemble into parallel arrangement [42].

### 2.3. X-ray diffraction measurements

The supramolecular self-assembly of dibenzophenazine based DLCs is investigated by X-ray diffraction studies using mesogenic compounds filled in a Lindemann capillaries. X-ray diffraction patterns were recorded for all the mesogens in the columnar mesophase both heating and subsequent cooling scan as shown in Fig. 3 and ESI Fig. S11. The diffraction parameters are summarized in Table 2. The mesogenic derivatives (**5**, **6a–6c**, **7a–7d** & **8a–8c**) exhibit increasing order of diffraction angle along with  $d$ -spacings of the highest intensity peak in the small angle region to the second one are in the ratio of 1:1/ $\sqrt{3}$ :1/2 respectively. These  $d$ -spacing values are obtained for the occurrence of hexagonal

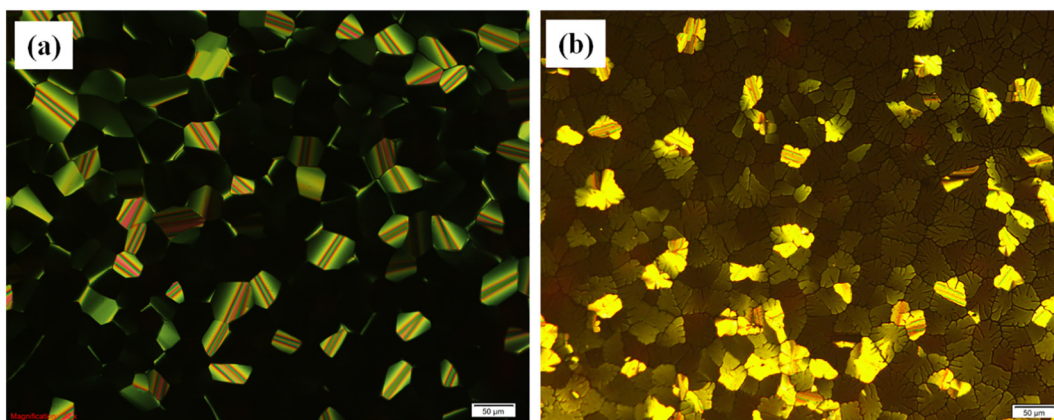


**Fig. 1.** Polarised optical micrographs taken in the hexagonal columnar phase, upon cooling from the isotropic melt. (a) Compound **6a**, recorded at 109 °C, viewed at 200× magnifications. (b) Compound **7a**, recorded at 157 °C, viewed at 200× magnifications.

columnar phase. In the wide angle regime, a diffuse peak responsible for the packing arrangement of flexible molten aliphatic chains and a weak peak in the wide-angle region is responsible for distance between discotic cores in the columns. The distance between adjacent columns in the mesophase was calculated using the relation  $a = d_{10}/(\cos 30^\circ)$ , where  $d_{10}$  is the  $d$ -spacing of highest intensity peak occurred in the small angle regime is shown in Table 2. The XRD pattern obtained for intermediate compound **5** in the columnar phase as shown in Fig. 3a (on heating). In the small angle region, three reflections are observed with corresponding  $d$ -spacings of  $d_1 = 22.31$  Å,  $d_2 = 12.81$  Å and  $d_3 = 11.34$  Å with increasing order of diffraction angle. These values confirm the occurrence of two-dimensional hexagonal columnar phase and the calculated lattice parameter,  $a$ , is found to be 25.76 Å at 120 °C. The broad halo peak ( $d = 4.35$  Å) in the wide-angle region obtained for the packing arrangement of molten aliphatic chains. The intercolumnar distance is estimated to be  $a = 25.76$  Å (Fig. 3a) (Table 2). Similarly, the powder XRD pattern was recorded for alkyl thiol substituted tetraalkoxy dibenzophenazine DLCs (**6a–6c**). A representative and typical XRD pattern recorded for compound **6c** in the columnar phase at 90 °C upon cooling from isotropic liquid is shown in Fig. 3b. The diffraction peaks observed in the small angle region with decreasing order of  $d$ -spacings  $d_1 = 24.73$  Å,  $d_2 = 14.33$  Å and  $d_3 = 12.41$  Å along with lattice parameter  $a = 28.55$  Å corresponds to the two-dimensional hexagonal columnar mesophase. The diffused peaks observed at wide angle region  $d = 4.55$  Å corresponding to packing of aliphatic chains and weak peak at  $d = 3.46$  Å corresponds to core-core separation. The distance between adjacent columns is found to be  $a = 28.55$  Å. The XRD pattern and corresponding lattice parameters were shown in ESI Fig. S11 and Table 2, respectively. The 4-alkoxy phenylacetylene

substituted unsymmetrical tetraalkoxy dibenzophenazine DLCs (**7a–7d**) exhibit similar X-ray diffraction patterns. A representative X-ray diffraction pattern obtained for compound **7a**, recorded at 120 °C in columnar phase upon cooling from isotropic liquid, is shown in Fig. 3c. The X-ray diffractogram shows several diffraction peaks in the small angle regions with  $d$ -spacings of  $d_1 = 23.51$  Å,  $d_2 = 13.56$  Å and  $d_3 = 11.73$  Å along with lattice parameter  $a = 27.14$  Å which implies the occurrence of hexagonal columnar phase. The broad diffused peak at  $d = 4.58$  Å corresponds to packing arrangement of flexible aliphatic chains. The weak peak in wide angle region at  $d = 3.47$  Å is attributed to the core-core separation in the columns. The intercolumnar distance between neighbouring columns is found to be 27.14 Å. Further, similar diffraction pattern observed for the symmetrical substituted 4-alkoxy phenylacetylene substituted tetraalkoxy dibenzophenazine DLCs (**8a–8c**). As a representative X-ray diffractogram, recorded for **8c** compound at 110 °C upon heating in the mesophase, is shown in Fig. 3d. In the small angle region three prominent diffraction peaks were observed with  $d$ -spacing's of  $d_1 = 26.48$  Å,  $d_2 = 15.28$  Å and  $d_3 = 13.25$  Å along with lattice constant  $a = 30.57$  Å which are expected from a two dimensional hexagonal columnar phase. The weak peak at wide angle regime with  $d = 3.50$  Å suggests the core-core separation in the columns. The intercolumnar distance between adjacent columns is estimated to be 30.57 Å. The above X-ray diffraction investigations reveal that all the discotic mesogens (**5**, **6a–c**, **7a–7d** & **8a–8c**) exhibit self-assembled hexagonal columnar mesophase structure where disc shape mesogens are stacked one on top of the other to form columns surrounding by flexible aliphatic chains. It is apparent that the intercolumnar distance between adjacent columns varies depending on the central core structure and length of flexible chains.

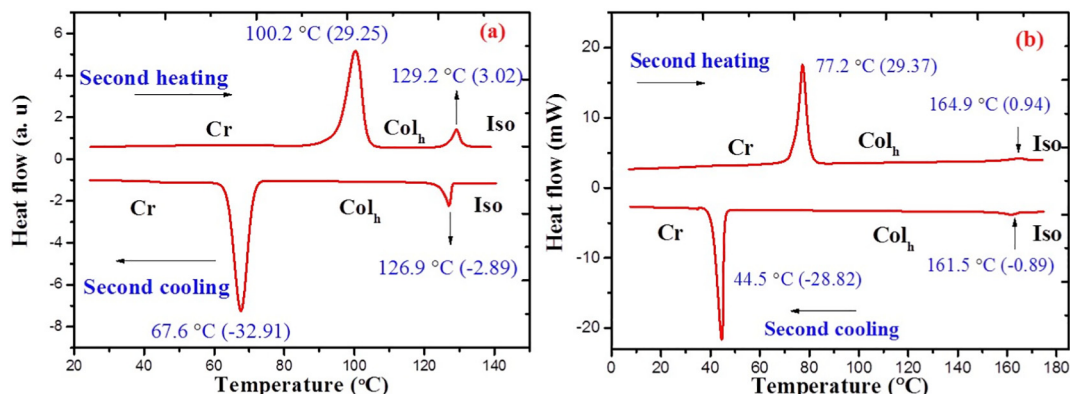


**Fig. 2.** DSC thermograms of (a) compound **6c** and (b) compound **8b**.

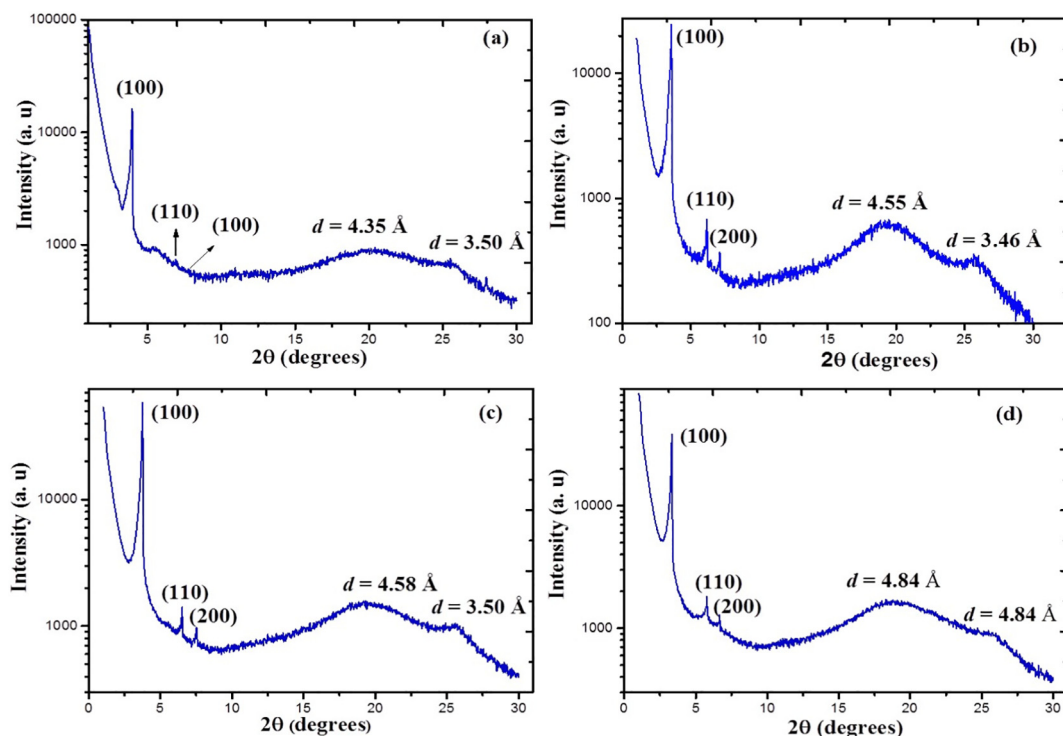


**Fig. 3.** XRD profiles showing the intensity against the  $2\theta$  recorded in the  $\text{Col}_h$  phase upon cooling from isotropic liquid. (a) Compound **5**, recorded at  $120^\circ\text{C}$ . (b) Compound **6c**, recorded at  $90^\circ\text{C}$ . (c) Compound **7a**, recorded at  $120^\circ\text{C}$ . (d) Compound **8c**, recorded at  $110^\circ\text{C}$ .

#### 2.4. Photophysical and self assemble properties

All the discotic mesogens (**6a–6c**, **7a–7d** and **8a–8c**) exhibit strong absorption and photo induced light emission properties. The UV–vis

absorption properties of all the mesogens were investigated using chloroform ( $10^{-5}$  M) solvent at ambient temperature to know absorption maxima as presented in Fig. 4 and corresponding absorption values are summarized in the Table 3. All the mesogens exhibit absorption

**Table 2**

XRD data of discotic mesogens (**5**, **6a–c**, **7a–7d** & **8a–8c**). The upper script a = on heating scan and b = on cooling scan.

Compound	Temperature ( $^\circ\text{C}$ ) <sup>a/b</sup>	$2\theta$ (degrees)	$d$ -Spacings/ $\text{\AA}$ observed (calculated)	Miller indexes	Phase/lattice constant	Alkyl-chain length ( $\text{\AA}$ )	Core-core separation ( $\text{\AA}$ )	Intercolumnar distance (a) ( $\text{\AA}$ )
<b>5</b>	120 <sup>a</sup>	3.96	22.31 (22.30)	100	$\text{Col}_h$ $a = 25.76$	4.35	3.50	25.76
		6.90	12.81 (12.88)	110				
		7.79	11.34 (11.15)	200				
<b>6a</b>	115 <sup>b</sup>	3.80	23.26 (23.25)	100	$\text{Col}_h$ $a = 26.85$	4.47	3.48	26.85
		6.56	13.46 (13.42)	110				
		7.58	11.66 (11.62)	200				
<b>6b</b>	85 <sup>a</sup>	3.70	23.91 (23.90)	100	$\text{Col}_h$ $a = 27.60$	4.50	3.43	27.60
		6.40	13.79 (13.80)	110				
		7.40	11.93 (11.95)	200				
<b>6c</b>	90 <sup>b</sup>	3.56	24.73 (24.72)	100	$\text{Col}_h$ $a = 28.55$	4.55	3.46	28.55
		6.16	14.33 (14.27)	110				
		7.11	12.41 (12.36)	200				
<b>7a</b>	120 <sup>b</sup>	3.75	23.51 (23.50)	100	$\text{Col}_h$ $a = 27.14$	4.58	3.47	27.14
		6.50	13.56 (13.57)	110				
		7.53	11.73 (11.75)	200				
<b>7b</b>	110 <sup>b</sup>	3.67	24.06 (24.05)	100	$\text{Col}_h$ $a = 27.78$	4.40	3.48	27.78
		6.37	13.84 (13.89)	110				
		7.35	12.03 (12.02)	200				
<b>7c</b>	65 <sup>a</sup>	3.59	24.55 (24.54)	100	$\text{Col}_h$ $a = 28.34$	4.45	3.51	28.34
		6.24	14.15 (14.17)	110				
		7.21	12.24 (12.27)	200				
<b>7d</b>	110 <sup>a</sup>	3.59	24.60 (24.59)	100	$\text{Col}_h$ $a = 28.40$	4.63	3.46	28.40
		6.24	14.15 (14.20)	110				
		7.21	12.24 (12.29)	200				
<b>8a</b>	100 <sup>b</sup>	3.56	24.73 (24.72)	100	$\text{Col}_h$ $a = 28.55$	4.52	3.50	28.55
		6.22	14.19 (14.27)	110				
		7.19	12.27 (12.36)	200				
<b>8b</b>	100 <sup>a</sup>	3.41	25.87 (25.86)	100	$\text{Col}_h$ $a = 29.87$	4.65	3.48	29.87
		5.90	14.95 (14.93)	110				
		6.82	12.94 (12.93)	200				
<b>8c</b>	110 <sup>a</sup>	3.33	26.48 (26.47)	100	$\text{Col}_h$ $a = 30.57$	4.84	3.50	30.57
		5.77	15.28 (15.28)	110				
		6.66	13.25 (13.23)	200				

bands below 463 nm. The alkylthiol substituted dibenzophenazine compounds (**6a–6c**) exhibit absorption bands at  $\lambda_{\max} = 451$  nm. Similarly, the unsymmetrical substituted phenylacetylene based dibenzophenazine derivatives (**7a–7d**) show maximum absorption band at  $\lambda_{\max} = 447$  nm and symmetrical substituted phenylacetylene based dibenzophenazine derivatives (**8a–8c**) exhibit absorption at longer wavelength at  $\lambda_{\max} = 463$  nm. The highly  $\pi$ -conjugated electronic systems and  $\pi$ - $\pi^*$  transitions in the dibenzophenazine heteroaromatic core, extended alkoxy phenylacetylene rings and the high molar absorption coefficients ( $\epsilon = 2$ – $2.77 \times 10^6$  L mol $^{-1}$  cm $^{-1}$  for compounds (**6a–6c**),  $\epsilon = 1.98$ – $3.69 \times 10^6$  L mol $^{-1}$  cm $^{-1}$  for compounds (**7a–7d**) and  $\epsilon = 2.95$ – $3.70 \times 10^6$  L mol $^{-1}$  cm $^{-1}$  for compounds (**8a–8c**)), are attributed to the maximum absorption in these  $\pi$ -extended dibenzophenazine based discotic liquid crystals. Generally, the extent of light absorption and intensity of the peaks in the absorption spectrum largely rely on the number of molecules that absorb light of a given wavelength. It is also known that extended conjugation in symmetrical substitution of 4-alkoxy phenylacetylene substituted phenazine derivatives (**8a–8c**) causes bathochromic shift (longer wavelength) with respect to the unsymmetrical substituted 4-alkoxy phenylacetylene derivatives (**7a–7d**) and alkylthiol substituted dibenzophenazine compounds (**6a–6c**). Similarly, photoluminescence emission studies of all the mesogens (**6a–6c**, **7a–7d** & **8a–8c**) were recorded using dilute solution of anhydrous chloroform solvent at ambient temperature. The dilute solutions of discotic mesogens were excited at 450 nm and corresponding emission behaviour is shown in Fig. 4. The thiol substituted discotic mesogens exhibit emission properties around 578–580 nm while symmetrical and unsymmetrical phenazine derivatives exhibit high emission properties around 597–600 nm (Table 3).

### 3. Thermogravimetric analysis

The thermal stability of novel discotic mesogens was investigated by thermogravimetric analysis (TGA) as shown in Fig. 5. All the samples

**Table 3**

The photophysical properties of discotic mesogens (**6a–6c**, **7a–7d** & **8a–8c**) recorded in anhydrous chloroform solvent ( $10^{-5}$  M).

Compound	Absorption ( $\lambda_{\max}/\text{nm}$ ) ( $\epsilon/10^6$ L mol $^{-1}$ cm $^{-1}$ )	Emission/nm
<b>6a</b>	450 (2.0)	578
<b>6b</b>	451 (2.35)	580
<b>6c</b>	450 (2.77)	580
<b>7a</b>	447 (2.83)	601
<b>7b</b>	446 (1.98)	599
<b>7c</b>	446 (3.69)	597
<b>7d</b>	447 (3.77)	599
<b>8a</b>	462 (3.70)	600
<b>8b</b>	463 (3.41)	599
<b>8c</b>	463 (2.95)	600

(**6a–6c**, **7a–7d** and **8a–8c**) were subjected to a heat scan of  $10$  °C min $^{-1}$  under a nitrogen atmosphere. The discotic mesogens (**6a–6c**) were thermally stable till  $330$  °C and initiated weight loss at about  $330$  °C– $340$  °C and decomposes at  $485$  °C. Similarly, symmetrical and unsymmetrical substituted phenazine discotic mesogens (**7a–7d** & **8a–8c**) were thermally stable upto  $355$  °C and initiated weight loss around  $360$ – $370$  °C and decomposes at  $510$  °C. The decomposition temperature of  $\pi$ -extended discotic mesogens are greater than corresponding thiol substituted compounds. The results reveal that thermal stability of  $\pi$ -extended symmetrical and asymmetrical phenazine discotic (**7a–7d** & **8a–8c**) is higher in comparison to thiol substituted discotic mesogens (**6a–6c**) (Fig. 5). All the novel mesogens exhibit higher thermal stability than their isotropic temperature.

### 4. Experimental section

The intermediate compounds 4,5-dibromobenzene-1,2-diamine (**3**) and 1-ethynyl-4-alkoxybenzene were synthesised as reported [49,50] and confirmed by spectral and elemental analysis.

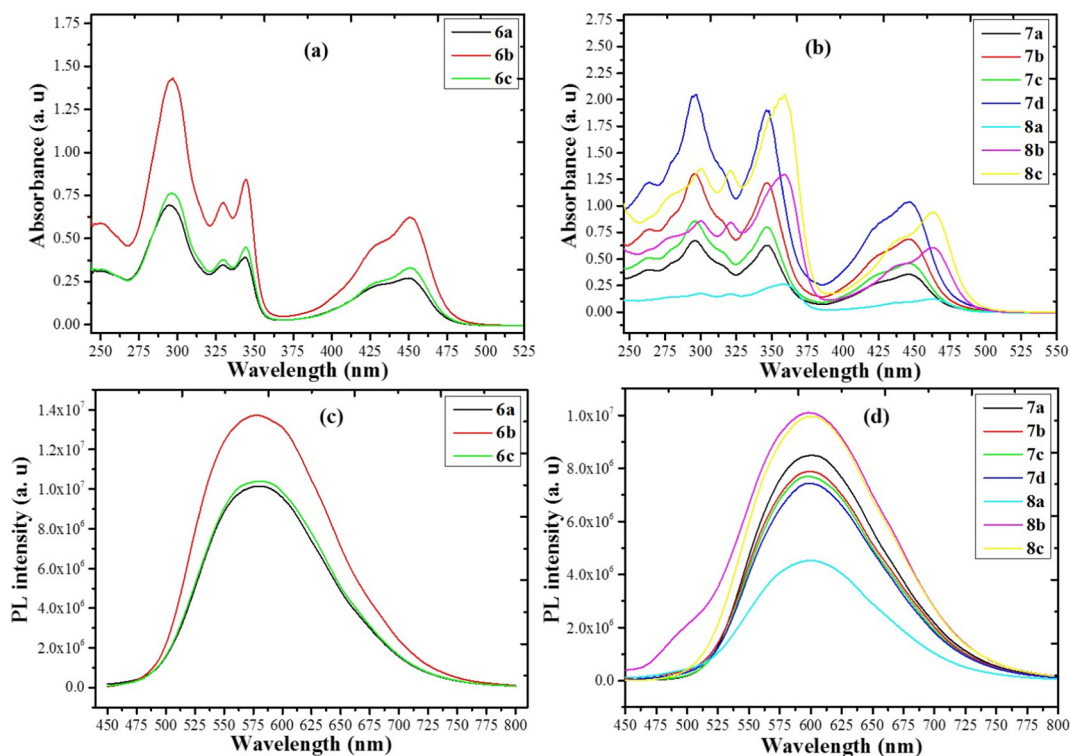


**Fig. 4.** (a) and (b) UV-Vis absorption spectra; (c) and (d) photoluminescence emission spectra of discotic mesogens (**6a–6c**, **7a–7d** & **8a–8c**).

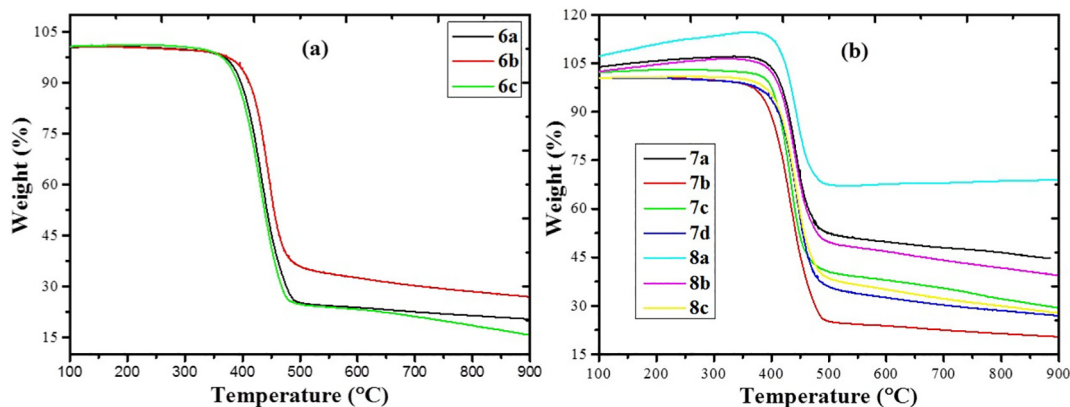


Fig. 5. Thermogravimetric analysis of compounds (6a–6c, 7a–7d & 8a–c).

#### 4.1. Synthesis of 1,2-bis(3,4-bis(dodecyloxy)phenyl)ethane-1,2-dione (**2**)

To a suspension of anhydrous aluminium chloride (0.29 g, 2.23 mmol) and 1,2-bis(dodecyloxy)benzene (2 g, 4.47 mmol) in dry dichloromethane (DCM) solvent (30 mL) under stirring, was added drop wise solution of oxalyl chloride (0.34 g, 2.68 mmol) in dry DCM solvent (10 mL) at 0 °C under nitrogen atmosphere. The resulting reaction mixture was stirred at the same temperature for 30 min and slowly allowed to room temperature for overnight. The reaction was quenched with 1 M aqueous HCl solution and extracted with DCM solvent (3 × 20 mL). The combined extract was dried over sodium sulphate (Na<sub>2</sub>SO<sub>4</sub>) and concentrated under reduced pressure. The crude compound was purified by column chromatography over silica gel (*n*-hexane: ethyl acetate, 9:1) and recrystallization with ethanol that gives pure compound **2** (Yield: 50%). IR (film)  $\nu_{\max}$ : 2918, 2906, 2852, 1664, 1583, 1462, 1377, 1265, 1074, 723 cm<sup>-1</sup>; <sup>1</sup>H NMR (500 MHz, CDCl<sub>3</sub>):  $\delta$  = 7.56 (s, 2H), 7.42 (d, 2H, *J* = 8.5 Hz), 6.84 (d, 2H, *J* = 8 Hz), 4.05 (t, 8H, 6 Hz), 1.83 (br, 8H), 1.46 (br, 8H), 1.35–1.26 (m, 64H), 0.88 ppm (t, 12H, *J* = 7 Hz); <sup>13</sup>C NMR (125 MHz, CDCl<sub>3</sub>):  $\delta$  = 193.78, 155.01, 149.33, 126.24, 126.09, 112.40, 111.65, 69.27, 69.14, 31.92, 29.70, 29.67, 29.65, 29.62, 29.58, 29.39, 29.36, 29.09, 28.94, 26, 25.93, 22.68, 14.10 ppm, elemental analysis: C<sub>62</sub>H<sub>106</sub>O<sub>6</sub>, calculated: C, 78.59; H, 11.28. % found: C, 78.48; H, 11.09. <sup>1</sup>H and <sup>13</sup>C NMR spectra are shown in the ESI, Fig. S12.

#### 4.2. Synthesis of 2,3-bis(3,4-bis(dodecyloxy)phenyl)-6,7-dibromoquinoxaline (**4**)

A mixture of compound **2** (1 g, 1.05 mmol) and 4,5-dibromobenzene-1,2-diamine **3** (0.28 g, 1.06 mmol) in glacial acetic acid (20 mL) was refluxed for overnight under nitrogen atmosphere [55]. After the completion of reaction, the reaction mixture was poured into ice cold water and extracted with DCM (3 × 20 mL). The organic layer was dried over Na<sub>2</sub>SO<sub>4</sub> and concentrated under reduced pressure. The crude compound was purified by column chromatography using silica gel (*n*-hexane: ethyl acetate, 7:3) and recrystallization with ethanol to give pure compound (**3**). Yield: 85%. IR (film)  $\nu_{\max}$ : 2949, 2920, 2899, 1600 1518, 1454, 1377, 1269, 1139, 721 cm<sup>-1</sup>; <sup>1</sup>H NMR (500 MHz, CDCl<sub>3</sub>):  $\delta$  = 8.42 (s, 2H), 7.08 (m, 4H), 6.82 (d, *J* = 8.5 Hz, 2H), 3.99 (t, *J* = 6.5 Hz, 4H), 3.82 (t, *J* = 6.5 Hz, 4H), 1.84–1.82 (m, 4H), 1.80–1.69 (m, 4H), 1.47–1.26 (m, 72H), 0.88 ppm (t, *J* = 6 Hz, 12H); <sup>13</sup>C NMR (125 MHz, CDCl<sub>3</sub>):  $\delta$  = 154.27, 150.33, 148.76, 140.23, 133, 131.06, 125.72, 122.92, 115.22, 113.06, 69.22, 69.18, 31.94, 31.80, 30.89, 30.04, 29.77, 29.71, 29.68, 29.66, 29.47, 29.43, 29.40, 29.38, 29.23, 29.15, 26.35, 26.04, 22.83, 22.70, 22.56, 14.11 ppm, elemental analysis: C<sub>68</sub>H<sub>108</sub>N<sub>2</sub>Br<sub>2</sub>O<sub>6</sub>, calculated: C, 69.37; H, 9.25; N, 2.38. % found: C, 69.21; H, 9.05; N, 2.21. <sup>1</sup>H and <sup>13</sup>C NMR spectra are shown in the ESI, Fig. S13.

#### 4.3. Synthesis of 11,12-dibromo-2,3,6,7-tetrakis(dodecyloxy)dibenzo[*a,c*]phenazine (**5**)

To a suspension of iron chloride (0.68 g, 4.24 mmol) in DCM solvent (20 mL) under stirring was added dropwise solution of compound **4** (1 g, 0.84 mmol) in DCM solvent (10 mL) at 0 °C under nitrogen atmosphere [56]. The reaction mixture was stirred at ambient temperature for 30 min. The reaction mixture was quenched with methanol and water. The resulting reaction mixture was extracted with DCM solvent (3 × 20 mL). The organic layer was dried over Na<sub>2</sub>SO<sub>4</sub> and concentrated under reduced pressure. The crude compound was purified by column chromatography using silica gel (*n*-hexane: ethyl acetate, 7:3) gives desired compound **5**. Yield: 80%. IR (film)  $\nu_{\max}$ : 2926, 2914, 2895, 1606, 1454, 1377, 1271, 1168, 1072, 721 cm<sup>-1</sup>; <sup>1</sup>H NMR (500 MHz, CDCl<sub>3</sub>):  $\delta$  = 8.45 (br, 4H), 7.49 (s, 2H), 4.15 (t, *J* = 6 Hz, 8H), 1.90 (t, *J* = 6.5 Hz, 8H), 1.61–1.52 (m, 8H), 1.61–1.20 (m, 64H), 0.80 ppm (t, *J* = 6.5 Hz, 12H); <sup>13</sup>C NMR (125 MHz, CDCl<sub>3</sub>):  $\delta$  = 152.09, 149.27, 142.36, 140.37, 132.89, 126.69, 124.79, 122.97, 108.55, 105.92, 69.46, 69.07, 31.95, 30.90, 29.78, 29.77, 29.75, 29.74, 29.71, 29.59, 29.40, 29.37, 26.24, 26.21, 22.70, 14.10 ppm, elemental analysis: C<sub>68</sub>H<sub>106</sub>N<sub>2</sub>Br<sub>2</sub>O<sub>2</sub>, calculated: C, 69.49; H, 9.09; N, 2.38. % found: C, 69.37; H, 8.95; N, 2.26. <sup>1</sup>H and <sup>13</sup>C NMR spectra are shown in the ESI, Fig. S14.

#### 4.4. Synthesis of 2,3,6,7-tetrakis(dodecyloxy)-11,12-bis(alkylthio)dibenzo[*a,c*]phenazine (**6a–6c**)

To a solution of intermediate compound **5** (0.5 g, 1 equiv) and anhydrous cesium carbonate (5 equiv) in dry *N,N*-dimethylacetamide solvent (DMAc) (20 mL) under stirring was added alkanethiol (2.2 equiv). The resulting reaction mixture was refluxed for 24 h. After cooling to room temperature, ice cold water was added and extracted with DCM solvent (3 × 20 mL). The combined extracts were dried over Na<sub>2</sub>SO<sub>4</sub> and concentrated under reduced pressure gives crude compound. The residue was purified by column chromatography using silica gel (*n*-hexane/DCM 9:1) which affords pure compound. Recrystallization of the pure product with cold ethanol gives final desired compound (**6a–6c**) in about 65% yield.

##### 4.4.1. 2,3,6,7-Tetrakis(dodecyloxy)-11,12-bis(hexylthio)dibenzo[*a,c*]phenazine (**6a**)

IR (film)  $\nu_{\max}$ : 2953, 2922, 2852, 1608, 1508, 1454, 1377, 1271, 1166, 771 cm<sup>-1</sup>; <sup>1</sup>H NMR (500 MHz, CDCl<sub>3</sub>):  $\delta$  = 8.63 (s, 2H), 7.90 (s, 2H), 7.62 (s, 2H), 4.25 (br, 4H), 4.18 (br, 4H), 3.11 (t, *J* = 7 Hz, 4H), 1.89 (br, 8H), 1.78–1.19 (br, 88H), 0.80 ppm (t, *J* = 6.5 Hz, 18H); <sup>13</sup>C NMR (125 MHz, CDCl<sub>3</sub>):  $\delta$  = 151.58, 149.44, 141.12, 140.19, 140.03, 129.46, 126.65, 126.33, 124.28, 123.89, 108.53, 106.48, 69.65, 69.15, 33.42, 32.60, 31.94, 31.42, 31.38, 30.90, 30.01, 29.75, 29.71, 29.70,

29.55, 29.43, 29.39, 28.84, 28.70, 28.63, 28.25, 26.22, 26.18, 22.70, 22.55, 14.11, 14.04 ppm; elemental analysis:  $C_{80}H_{132}N_2O_4S_2$ , calculated: C, 76.87; H, 10.64; N, 2.24; S, 5.13, % found: C, 76.77; H, 10.56; N, 2.31; S, 4.91.  $^1H$  and  $^{13}C$  NMR spectra are shown in the ESI, Fig. S15.

#### 4.4.2. 2,3,6,7-Tetrakis(dodecyloxy)-11,12-bis(octylthio)dibenzo[a,c]phenazine (**6b**)

IR (film)  $\nu_{max}$ : 2953, 2920, 2852, 1608, 1504, 1462, 1377, 1271, 1166, 767  $cm^{-1}$ ;  $^1H$  NMR (500 MHz,  $CDCl_3$ ):  $\delta$  = 8.65 (s, 2H), 7.92 (s, 2H), 2 (s, 2H), 4.27 (br, 4H), 4.19 (br, 4H), 3.13 (t,  $J$  = 7 Hz, 4H), 1.89 (br, 8H), 1.79–1.20 ppm (m, 96H), 0.80 (m, 18H);  $^{13}C$  NMR (125 MHz,  $CDCl_3$ ):  $\delta$  = 151.61, 149.46, 141.17, 140.23, 140.07, 126.35, 124.34, 123.92, 108.56, 106.53, 69.66, 69.17, 33.45, 31.94, 31.82, 30.91, 29.75, 29.69, 29.54, 29.42, 29.39, 29.20, 29.19, 29.17, 28.29, 26.21, 26.18, 22.69, 14.11, 14.09 ppm; elemental analysis:  $C_{84}H_{140}N_2O_4S_2$ , calculated: C, 77.24; H, 10.80; N, 2.14; S, 4.91, % Found: C, 77.34; H, 10.96; N, 2.23; S, 5.06.  $^1H$  and  $^{13}C$  NMR spectra are shown in the ESI, Fig. S16.

#### 4.4.3. 2,3,6,7-Tetrakis(dodecyloxy)-11,12-bis(dodecylthio)dibenzo[a,c]phenazine (**6c**)

IR (film)  $\nu_{max}$ : 2953, 2918, 2850, 1608, 1510, 1462, 1377, 1271, 1166, 1074, 721  $cm^{-1}$ ;  $^1H$  NMR (500 MHz,  $CDCl_3$ ):  $\delta$  = 8.67 (s, 2H), 7.94 (s, 2H), 7.67 (s, 2H), 4.28 (br, 4H), 4.20 (br, 4H), 3.14 (t,  $J$  = 6.5 Hz, 4H), 1.89 (br, 8H), 1.81–1.19 (m, 112H), 0.80 ppm (br, 18H);  $^{13}C$  NMR (125 MHz,  $CDCl_3$ ):  $\delta$  = 151.85, 151.60, 149.27, 141.83, 141.25, 140.58, 139.47, 132.06, 131.22, 130.39, 126.66, 126.16, 123.49, 108.59, 106.08, 69.52, 69.12, 69.03, 33.17, 29.78, 29.61, 29.41, 27.85, 22.71, 14.11 ppm; elemental analysis:  $C_{92}H_{156}N_2O_4S_2$ , calculated: C, 77.91; H, 11.09; N, 1.98; S, 4.52, % Found: C, 77.79; H, 11.25; N, 2.18; S, 4.65.  $^1H$  and  $^{13}C$  NMR spectra are shown in the ESI, Fig. S17.

#### 4.5. Synthesis of symmetrical and unsymmetrical dibenzophenazine based discotic mesogen (**7a–7d** and **8a–8c**)

All the final discotic mesogens were obtained by Sonogashira C—C bond coupling reaction between 11,12-dibromo-2,3,6,7-tetrakis(dodecyloxy)dibenzo[a,c]phenazine (**5**) with 1-ethynyl-4-alkoxybenzene in the presence of  $PdCl_2(PPh_3)_2$  and CuI in anhydrous triethylamine solvent [57,58]. The general method is described as follows.

To a mixture of bis(triphenylphosphine) palladium dichloride (0.04 eq.) and CuI (0.06 eq.) was added compound **5** (0.5 g, 1 eq.) in anhydrous triethylamine solvent under nitrogen atmosphere and allowed to stir at room temperature for 10 min. To the above reaction mixture, 1-ethynyl-4-(alkoxy)benzene (1.2 eq.) in anhydrous triethylamine was added under nitrogen flow. The resulting reaction mixture was heating to 75 °C for 24 h. The residue was diluted with diethyl ether and filtered through celite pad. The filtrate was washed with water and then extracted with diethyl ether (3 × 40 mL). The combined extracts were dried over  $Na_2SO_4$  and concentrated under reduced pressure. The crude compound was purified by column chromatography using silica gel (hexane: ethylacetate 8:2) gives desired compound **7a–7d**. Similarly, symmetrical discotic mesogens (**8a–8c**) were obtained by using compound **5** (0.5 g, 1 eq.),  $PdCl_2(PPh_3)_2$  (0.08 eq.), CuI (0.09 eq.) and 1-ethynyl-4-(alkoxy)benzene (2.5 eq.) respectively.

#### 4.5.1. 11-Bromo-12-((4-butoxyphenyl)ethynyl)-2,3,6,7-tetrakis(dodecyloxy)dibenzo[a,c]phenazine (**7a**)

IR (film)  $\nu_{max}$ : 2951, 2924, 2852, 2214, 1606, 1510, 1454, 1377, 1273, 1166, 773, 721  $cm^{-1}$ ;  $^1H$  NMR (500 MHz,  $CDCl_3$ ):  $\delta$  = 8.52 (s, 1H), 8.49 (s, 1H), 8.43 (s, 1H), 8.34 (s, 1H), 7.61 (d,  $J$  = 8 Hz, 2H), 7.50 (br, 2H), 6.95 (d,  $J$  = 8 Hz, 2H), 4.29–4.24 (br, 8H), 4.03 (t,  $J$  = 5.5 Hz, 2H), 2.0 (br, 8H), 1.83–1.30 (m, 76H), 1.03 (t,  $J$  = 6.5 Hz, 3H), 0.98 ppm (br, 12H);  $^{13}C$  NMR (125 MHz,  $CDCl_3$ ):  $\delta$  = 159.82, 152, 151.89, 149.29, 149.25, 142.33, 142.04, 141.07, 139.95, 133.36, 132.70, 131.99, 126.70, 126.51, 125.88, 124.97, 123.28, 123.19, 114.68, 108.61,

106.05, 96.12, 87.13, 69.51, 69.08, 67.84, 31.95, 31.26, 29.78, 29.72, 29.60, 29.41, 26.24, 26.21, 22.70, 19.25, 14.11, 13.85 ppm; elemental analysis:  $C_{80}H_{119}N_2BrO_5$ , calculated: C, 75.73; H, 9.45; N, 2.21. % Found: C, 75.66; H, 9.36, 2.29.  $^1H$  and  $^{13}C$  NMR spectra are shown in the ESI, Fig. S18.

#### 4.5.2. 11-Bromo-2,3,6,7-tetrakis(dodecyloxy)-12-((4-(octyloxy)phenyl)ethynyl)dibenzo[a,c]phenazine (**7b**)

IR (film)  $\nu_{max}$ : 2953, 2922, 2852, 2210, 1606, 1511, 1456, 1375, 1271, 1166, 771, 721  $cm^{-1}$ ;  $^1H$  NMR (500 MHz,  $CDCl_3$ ): 8.38–8.33 (m, 3H), 8.22 (s, 1H), 7.58 (d,  $J$  = 7 Hz, 2H), 7.37 (br, 2H), 6.91 (d,  $J$  = 7 Hz, 2H), 4.21 (br, 8H), 3.99 (br, 2H), 1.96 (br, 8H), 1.81–1.28 (m, 84H), 0.86 ppm (br, 15H);  $^{13}C$  NMR (125 MHz,  $CDCl_3$ ):  $\delta$  = 159.80, 151.89, 151.78, 149.15, 149.10, 142.16, 141.87, 140.95, 139.82, 133.35, 132.65, 131.92, 126.57, 126.38, 125.71, 124.82, 123.13, 123.03, 114.73, 114.68, 108.48, 105.81, 105.68, 87.17, 69.42, 69.38, 69.03, 68.17, 31.96, 31.84, 29.80, 29.74, 29.71, 29.65, 29.43, 29.26, 29.24, 26.27, 26.23, 26.06, 22.71, 22.68, 14.12 ppm; elemental analysis:  $C_{84}H_{127}N_2BrO_5$ , calculated: C, 76.15; H, 9.66; N, 2.11. % Found: C, 76.26; H, 9.78, N, 2.23.  $^1H$  and  $^{13}C$  NMR spectra are shown in the ESI, Fig. S19.

#### 4.5.3. 11-Bromo-2,3,6,7-tetrakis(dodecyloxy)-12-((4-(tetradecyloxy)phenyl)ethynyl)dibenzo[a,c]phenazine (**7c**)

IR (film)  $\nu_{max}$ : 2953, 2920, 2866, 2216, 1606, 1506, 1456, 1377, 1271, 1168, 771, 721  $cm^{-1}$ ;  $^1H$  NMR (500 MHz,  $CDCl_3$ ): 8.53–8.49 (br, 2H), 8.43 (s, 1H), 8.34 (s, 1H), 7.58 (d,  $J$  = 8 Hz, 2H), 7.51 (br, 2H), 6.92 (d,  $J$  = 8 Hz, 2H), 4.25 (br, 8H), 3.99 (t,  $J$  = 6 Hz, 2H), 2.01–1.93 (m, 8H), 1.84–1.27 (m, 96H), 0.88 ppm (t,  $J$  = 6.5 Hz, 15H);  $^{13}C$  NMR (125 MHz,  $CDCl_3$ ):  $\delta$  = 159.82, 152, 151.89, 149.25, 142.04, 141.07, 139.95, 133.36, 132.68, 131.98, 126.70, 126.50, 125.88, 124.98, 123.27, 123.19, 114.68, 114.68, 108.57, 106.06, 96.13, 87.13, 69.48, 69.07, 68.18, 31.95, 29.78, 29.72, 29.61, 29.41, 29.37, 29.23, 26.24, 26.05, 22.70, 14.11 ppm; elemental analysis:  $C_{90}H_{139}N_2BrO_5$ , calculated: C, 76.72; H, 9.94; N, 1.99. % Found: C, 76.84; H, 10.10; N, 2.13.  $^1H$  and  $^{13}C$  NMR spectra are shown in the ESI, Fig. S20.

#### 4.5.4. 11-Bromo-12-((4-((3,7-dimethyloctyl)oxy)phenyl)ethynyl)-2,3,6,7-tetrakis(dodecyloxy)dibenzo[a,c]phenazine (**7d**)

IR (film)  $\nu_{max}$ : 2951, 2922, 2852, 2210, 1608, 1506, 1456, 1375, 1271, 1168, 771, 721  $cm^{-1}$ ;  $^1H$  NMR (500 MHz,  $CDCl_3$ ): 8.40 (s, 1H), 8.37 (s, 1H), 8.31 (s, 1H), 8.23 (s, 1H), 7.51 (d,  $J$  = 7.5 Hz, 2H), 7.38 (br, 2H), 6.85 (d,  $J$  = 7.5 Hz, 2H), 4.16 (m, 8H), 3.97 (br, 2H), 1.90 (m, 8H), 1.8–1.2 (m, 82H), 0.90 (d,  $J$  = 6 Hz, 3H), 0.81 ppm (br, 18H);  $^{13}C$  NMR (125 MHz,  $CDCl_3$ ):  $\delta$  = 159.80, 151.98, 151.87, 149.26, 149.22, 142.30, 142.01, 141.06, 139.93, 133.36, 132.69, 131.98, 126.68, 126.48, 125.85, 124.94, 126.26, 123.16, 114.69, 108.58, 106, 105.89, 96.11, 87.14, 69.49, 69.45, 69.07, 66.51, 39.27, 37.33, 36.15, 31.96, 29.90, 29.78, 29.75, 29.72, 29.62, 29.41, 27.99, 26.25, 26.21, 24.68, 22.71, 22.61, 19.67, 14.11 ppm; elemental analysis:  $C_{86}H_{131}N_2BrO_5$ , calculated: C, 76.35; H, 9.76; N, 2.07. % Found: C, 76.25; H, 9.64; N, 1.98.  $^1H$  and  $^{13}C$  NMR spectra are shown in the ESI, Fig. S21.

#### 4.5.5. 11,12-Bis((4-butoxyphenyl)ethynyl)-2,3,6,7-tetrakis(dodecyloxy)dibenzo[a,c]phenazine (**8a**)

IR (film)  $\nu_{max}$ : 2955, 2922, 2852, 2216, 1606, 1506, 1456, 1377, 1269, 1168, 771, 721  $cm^{-1}$ ;  $^1H$  NMR (500 MHz,  $CDCl_3$ ): 8.62 (br, 2H), 8.39 (br, 2H), 7.59 (m, 6H), 6.93 (d,  $J$  = 8 Hz, 4H), 4.32–4.26 (m, 8H), 4.03 (t,  $J$  = 6.5 Hz, 4H), 1.99 (t,  $J$  = 6 Hz, 8H), 1.83–1.30 (m, 80H), 1.03 (t,  $J$  = 7 Hz, 6H), 0.89 ppm (br, 12H);  $^{13}C$  NMR (125 MHz,  $CDCl_3$ ):  $\delta$  = 159.61, 151.88, 149.36, 142.23, 140.73, 133.34, 131.85, 126.57, 125.83, 123.59, 115.15, 114.65, 108.69, 106.23, 95.39, 87.20, 69.57, 69.10, 67.83, 31.94, 31.28, 29.77, 29.71, 29.58, 29.40, 26.20, 22.70, 19.25, 14.11, 13.85 ppm; elemental analysis:  $C_{92}H_{132}N_2O_6$ , calculated: C, 81.13; H, 9.77; N, 2.06. % Found: C, 81.26; H, 9.86; N, 2.18.  $^1H$  and  $^{13}C$  NMR spectra are shown in the ESI, Fig. S22.

#### 4.5.6. 2,3,6,7-Tetrakis(dodecyloxy)-11,12-bis((4-(octyloxy)phenyl)ethynyl)dibenzo[a,c]phenazine (**8b**)

IR (film)  $\nu_{\max}$ : 2953, 2924, 2852, 2208, 1606, 1507, 1456, 1377, 1247, 1168, 769, 721  $\text{cm}^{-1}$ ;  $^1\text{H}$  NMR (500 MHz,  $\text{CDCl}_3$ ): 8.56 (br, 2H), 8.33 (br, 2H), 7.57–7.52 (m, 6H), 6.90 (d,  $J = 7$  Hz, 4H), 4.29–4.22 (m, 8H), 3.99 (br, 4H), 1.97 (br, 8H), 1.81–1.27 (m, 96H), 0.88 ppm (br, 18H);  $^{13}\text{C}$  NMR (125 MHz,  $\text{CDCl}_3$ ):  $\delta = 159.61, 151.83, 149.28, 142.15, 140.69, 133.33, 131.84, 126.54, 125.78, 123.50, 115.15, 114.65, 108.64, 106.14, 95.37, 87.21, 69.54, 69.09, 68.16, 31.95, 31.83, 29.77, 29.74, 29.72, 29.60, 29.40, 29.39, 29.25, 26.22, 26.20, 26.06, 22.70, 22.67, 14.10$  ppm; elemental analysis:  $\text{C}_{100}\text{H}_{148}\text{N}_2\text{O}_6$ , calculated: C, 81.47; H, 10.12; N, 1.90. % Found: C, 81.59; H, 10.23; N, 2.09.  $^1\text{H}$  and  $^{13}\text{C}$  NMR spectra are shown in the ESI, Fig. S23.

#### 4.5.7. 11,12-Bis((4-((3,7-dimethyloctyl)oxy)phenyl)ethynyl)-2,3,6,7-tetrakis(dodecyloxy)dibenzo[a,c]phenazine (**8c**)

IR (film)  $\nu_{\max}$ : 2953, 2920, 2852, 2218, 1606, 1506, 1456, 1377, 1246, 1168, 771, 721  $\text{cm}^{-1}$ ;  $^1\text{H}$  NMR (500 MHz,  $\text{CDCl}_3$ ): 8.44 (br, 2H), 8.25 (br, 2H), 7.57 (d,  $J = 7.5$  Hz, 4H), 7.39 (br, 2H), 6.90 (d,  $J = 7.5$  Hz, 4H), 4.26–4.19 (m, 8H), 4.03 (d,  $J = 5.5$  Hz, 4H), 1.98–1.19 (m, 100H), 0.97 (m, 6H), 0.88 ppm (br, 24H);  $^{13}\text{C}$  NMR (125 MHz,  $\text{CDCl}_3$ ):  $\delta = 159.57, 151.72, 149.13, 141.96, 140.56, 133.34, 131.84, 126.41, 125.60, 123.33, 115.23, 114.65, 108.51, 105.84, 95.26, 87.29, 69.43, 69.05, 66.49, 39.28, 37.35, 36.20, 31.97, 29.92, 29.80, 29.74, 29.66, 29.48, 29.43, 28, 26.27, 26.23, 24.69, 22.72, 22.62, 19.68, 14.12$  ppm; elemental analysis:  $\text{C}_{104}\text{H}_{156}\text{N}_2\text{O}_6$ , calculated: C, 81.62; H, 10.27; N, 1.83. % Found: C, 81.88; H, 10.41, 2.01.  $^1\text{H}$  and  $^{13}\text{C}$  NMR spectra are shown in the ESI, Fig. S24.

## 5. Conclusions

Several new dibenzophenazine based discotic liquid crystals containing alkanethiols, alkoxy phenylacetylene and alkoxy chains has been synthesised and characterized. The mesomorphic properties were characterized using polarised optical microscopy and differential scanning calorimetry. The columnar nature of the mesophase was investigated using X-ray diffraction method. The addition of alkoxythiol chains leads to an enhancement in the molecular dipole moment, which favours the parallel orientation of adjacent molecules within the columns. The isotropic temperature of alkoxythiol substituted DLCs is lower in comparison to  $\pi$ -extended alkoxyphenylacetylene and alkoxy compounds. The dibenzophenazine fused discotic liquid crystals containing  $\pi$ -extended alkoxy phenylacetylene and alkoxy chains self-organize into hexagonal columnar phase may be due to large size aromatic core. All the new  $\pi$ -extended dibenzophenazine based mesogens exhibit strong photoluminescence properties in the anhydrous chloroform solvent. The  $\pi$ -extended heteroaromatic discotic mesogens may play significant role in organic optoelectronic devices and solar cells applications.

## Declaration of competing interest

We declare that we don't have any conflict of interest.

## Acknowledgments

The author thanks Dr. Vijayaragavan for recording the NMR spectra, Dr. Srinivas HT and Ms. Vasuda for their technical support. Department of Science and Technology, Government of India, Grant INT/RUS/RFBR/376 and Russian Foundation for Basic Projects, grant No. 19-57-45011\_Ind\_a are gratefully acknowledged.

## Appendix A. Supplementary data

The general methods, POM images, DSC thermograms, XRD data,  $^1\text{H}$  NMR and  $^{13}\text{C}$  NMR spectra of intermediate and final compounds have

been provided in the supporting information. Supplementary data to this article can be found online at <https://doi.org/10.1016/j.molliq.2020.114419>.

## References

- [1] P.J. Collings, *Liquid Crystals: Nature's Delicate Phase of Matter*, Princeton University Press, Princeton, NJ, 1990.
- [2] T. Kato, N. Mizoshita, K. Kishimoto, *Angew. Chem. Int. Ed.* 45 (2006) 38–68.
- [3] S. Kumar, *Chem. Soc. Rev.* 35 (2006) 83–109.
- [4] M.T. Allen, S. Diele, K.D.M. Harris, T. Hegmann, B.M. Kariuki, D. Lose, J.A. Preece, C. Tschierske, *J. Mater. Chem.* 11 (2001) 302–311.
- [5] H. Iino, J.-i. Hanna, *J. Opto-Electron. Rev.* 13 (2005) 295–302.
- [6] H.K. Bisoyi, S. Kumar, *Chem. Soc. Rev.* 39 (2010) 264–285.
- [7] T. Wçhrle, I. Wurzbach, J. Kirres, A. Kostidou, N. Kapernaum, J. Litterscheidt, J.C. Haenle, P. Staffeld, A. Baro, F. Giesselmann, S. Laschat, *Chem. Rev.* 116 (2016) 1139–1241.
- [8] E.-K. Fleischmann, R. Zentel, *Angew. Chem. Int. Ed.* 52 (2013) 8810–8827.
- [9] J.P.F. Laggerwall, G. Scalia, *Curr. Appl. Phys.* 12 (2012) 1387–1412.
- [10] S. Kumar, *Isr. J. Chem.* 52 (2012) 820–829.
- [11] Q. Li, *Liquid Crystals Beyond Display: Chemistry, Physics and Applications*, John Wiley & Sons, 2012.
- [12] R.J. Bushby, O.R. Lozman, *Curr. Opin. Colloid Interface Sci.* 7 (2002) 343–354.
- [13] M. Bremer, P. Kirsch, M. Klases-Memmer, K. Tarumi, *Angew. Chem. Int. Ed.* 52 (2013) 8880–8896.
- [14] S. Kumar, *Chemistry of Discotic Liquid Crystals: From Monomers to Polymers*, CRC Press, Boca Raton, FL, 2010.
- [15] S. Kumar, Design concepts and synthesis of discotic liquid crystals, in: J.W. Goodby, P.J. Collings, T. Kato, C. Tschierske, H.F. Gleeson, P. Raynes (Eds.), *Handbook of Liquid Crystals*, vol. 4, Wiley-VCH, Weinheim, 2014.
- [16] S. Sergeev, W. Pisula, Y.H. Geerts, *Chem. Soc. Rev.* 36 (2007) 1902–1929.
- [17] H. Iino, J. Hanna, R.J. Bushby, B. Movaghar, B.J. Whitaker, M. Cook, *J. Appl. Phys. Lett.* 87 (2005) 132102.
- [18] A. Tracz, J.K. Jezka, M.D. Watson, W. Pisula, K. Müllen, T. Pakula, *J. Am. Chem. Soc.* 125 (2003) 1682–1683.
- [19] W. Pisula, Z. Tomovic, B. El Hamaoui, M.D. Watson, T. Pakula, K. Müllen, *Adv. Funct. Mater.* 15 (2005) 893–904.
- [20] O. Bunk, M.M. Nielsen, T.I. Solling, A.M. Van de Craats, N. Stutzmann, *J. Am. Chem. Soc.* 125 (2003) 2252–2258.
- [21] G.G. Nair, D.S.S. Rao, S.K. Prasad, S. Chandrasekhar, S. Kumar, *Mol. Cryst. Liq. Cryst.* 397 (2003) 245–252.
- [22] S. Kumar, S.K. Varshney, *Angew. Chem. Int. Ed.* 112 (2000) 3270–3272.
- [23] S. Kumar, *Pramana.* 61 (2003) 199–203.
- [24] H. Mori, Y. Itoh, Y. Nishuira, T. Nakamura, Y. Shinagawa, *Jpn. J. Appl. Phys.* 36 (1997) 143–147.
- [25] K. Kawata, *Chem. Rec.* 2 (2002) 59–80.
- [26] C. Destrade, N.H. Tinh, H. Gasparoux, J. Malthe, A.M. Levelut, *Mol. Cryst. Liq. Cryst.* 71 (1981) 111–135.
- [27] A. Bacher, I. Bleyl, C.H. Erdelen, D. Haarer, W. Paulus, H.-W. Schmidt, *Adv. Mater.* 9 (1997) 1031–1035.
- [28] I. Seguy, P. Jolinat, P. Destruel, J. Farenc, R. Mamy, H. Bock, J. Ip, T.P. Nguyen, *J. Appl. Phys.* 89 (2001) 5442–5448.
- [29] T. Hassheider, S.A. Benning, H.-S. Kitzerow, A.-F. Achardand, H. Bock, *Angew. Chem. Int. Ed.* 40 (2001) 2060–2063.
- [30] A.M. van de Craats, N. Stutzmann, O. Bunk, M.M. Nielsen, M. Watson, K. Müllen, H.D. Chanzhy, H. Siringhaus, R.H. Friend, *Adv. Mater.* 15 (2003) 495–499.
- [31] S. Cherian, C. Donley, D. Mathine, L. LaRussa, W. Xia, N. Armstrong, *J. Appl. Phys.* 96 (2004) 5638–5643.
- [32] S. Xiao, M. Myers, Q. Miao, S. Sanaur, K. Pang, M.L. Steigerwald, C. Nuckolls, *Angew. Chem. Int. Ed.* 44 (2005) 7390–7394.
- [33] J.-Y. Cho, B. Domercq, S.C. Jones, J. Yu, X. Zhang, Z. An, M. Bishop, S.R. Marder, B. Kippelen, *J. Mater. Chem.* 17 (2007) 2642–2647.
- [34] D. Adam, P. Schuhmacher, J. Simmerer, L. Haussling, K. Selemensmeyer, K.H. Etzbach, H. Ringsdorf, D. Haarer, *Nature* 371 (1994) 141–143.
- [35] M. Kumar, S. Kumar, *Polym. J.* 49 (2017) 85–111.
- [36] J. Clements, N. Boden, T.D. Gibson, R.C. Chandler, J.N. Hulbert, E.A. Ruck-Keene, *Sensors Actuators B Chem.* 47 (1998) 37–42.
- [37] J.D. Wright, P. Roisin, G.P. Rigby, R.J.M. Nolte, M.J. Cook, S.C. Thorpe, *Sens. Actuators E.* 13 (1993) 276–280.
- [38] M. Krishnaiah, N.R. de Almeida, V. Udumula, Z. Song, Y.S. Chhonker, M.M. Abdelmoaty, V.A. do Nascimento, D.J. Murry, M. Conda-Sheridan, *Eur. J. Med. Chem.* 143 (2018) 936–947.
- [39] L.S. Pierson, E.A. Pierson, *Appl. Microbiol. Biotechnol.* 86 (2010) 1659–1670.
- [40] A.M. Shaikh, B.K. Sharma, S. Chacko, R.M. Kamble, *New J. Chem.* 41 (2017) 628–638.
- [41] E.J. Foster, C. Lavigneur, Y.-C. Ke, V.E. Williams, *J. Mater. Chem.* 15 (2005) 4062–4068.
- [42] E.J. Foster, R.B. Jones, C. Lavigneur, V.E. Williams, *J. Am. Chem. Soc.* 126 (2006) 8569–8574.
- [43] C. Lavigneur, E.J. Foster, V.E. Williams, *J. Am. Chem. Soc.* 130 (2008) 11791–11800.
- [44] K.J.A. Bozek, V.E. Williams, *Soft Matter* 10 (2014) 5749–5754.
- [45] C.W. Ong, J.Y. Hwang, M.-C. Tzeng, S.-C. Liao, H.-F. Hsu, T.-H. Chang, *J. Mater. Chem.* 17 (2007) 1785–1790.
- [46] C.W. Ong, C.Q. Yan, M.-C. Yeh, M.-C. Tzeng, *Mol. Cryst. Liq. Cryst.* 610 (2015) 249–254.

- [47] J. Szydłowska, P. Krzyczkowska, M. Salamonczyk, E. Gorecka, D. Pocięcha, B. Maranowski, A. Krowczyński, *J. Mater. Chem. C* 1 (2013) 6883–6889.
- [48] K.-T. Lin, C.K. Lai, *Tetrahedron* 72 (2016) 7579–7588.
- [49] J. Shao, J. Chang, C. Chi, *Org. Biomol. Chem.* 10 (2012) 7045–7052.
- [50] Y. Arakawa, S. Nakajima, R. Ishige, M. Uchimura, S. Kang, G.-I. Konishi, J. Watanabe, *J. Mater. Chem.* 22 (2012) 8394–8398.
- [51] C.-Y. Liu, A. Fechtenkoetter, M.D. Watson, K. Mullen, A.J. Bard, *J. Chem. Mater.* 15 (2003) 124.
- [52] K. Lau, J. Foster, V. Williams, *Chem. Commun.* (2003) 2172.
- [53] A.N. Cammidge, H. Gopee, *Chem. Commun.* (2002) 966.
- [54] W. Pisula, Z. Tomovic, C. Simpson, M. Kastler, T. Pakula, K. Mullen, *Chem. Mater.* 17 (2005) 4296.
- [55] C.W. Ong, C.-Y. Hwang, S.-C. Liao, C.-H. Pan, T.-H. Chang, *J. Mater. Chem.* 19 (2009) 5149–5154.
- [56] A.A.O. Sarhanw, C. Bolm, *Chem. Soc. Rev.* 38 (2009) 2730–2744.
- [57] M.B. Rodrigues, R.A.P. Halfen, S.C. Feitosa, C.P. Frizzo, M.A.P. Martins, N. Zanatta, A.A. Merlo, H.G. Bonacorso, *J. Mol. Liq.* 287 (2019) 110896.
- [58] A. Tavares, P.R. Livotto, P.F.B. Gonçalves, A.A. Merlo, *J. Braz. Chem. Soc.* 20 (2009) 1742–1752.